

# Gradient-Informed Quality Diversity for the Illumination of Discrete Spaces

Raphaël Boige\*  
InstaDeep  
Paris, France  
r.boige@instadeep.com

Guillaume Richard\*  
InstaDeep  
Paris, France  
g.richard@instadeep.com

Jérémie Donà  
InstaDeep  
Paris, France  
j.dona@instadeep.com

Antoine Cully  
Imperial College London  
London, United Kingdom  
a.cully@imperial.ac.uk

Thomas Pierrot  
InstaDeep  
Boston, MA  
t.pierrot@instadeep.com

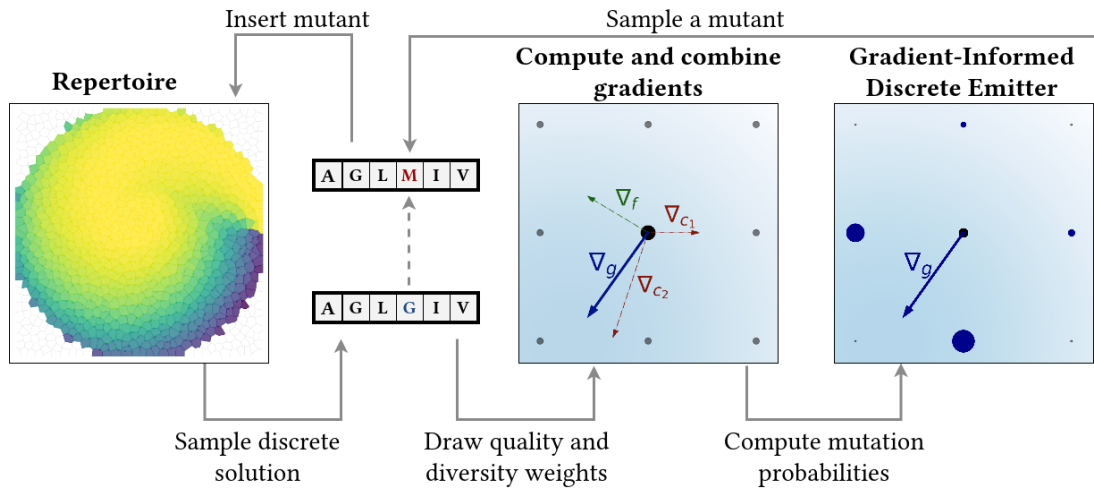


**Figure 1: MAP-Elites with Gradients Informed Discrete Emitter (ME-GIDE).** At each iteration, a discrete solution (here a sequence of letters from a finite vocabulary) is sampled in the repertoire. Gradients are computed over continuous fitness and descriptor functions with respect to their discrete inputs. Gradients are linearly combined to favour higher fitness and exploration of the descriptor space. Probabilities of mutation over the neighbours of the element are derived from this gradient information. Finally, a mutant is sampled according to those probabilities and inserted back in the repertoire.

## ABSTRACT

Quality Diversity (QD) algorithms have been proposed to search for a large collection of both diverse and high-performing solutions instead of a single set of local optima. While early QD algorithms view the objective and descriptor functions as black-box functions, novel tools have been introduced to use gradient information to accelerate the search and improve overall performance of those algorithms over continuous input spaces. However a broad range

\*Both authors contributed equally to this research.

Permission to make digital or hard copies of all or part of this work for personal or classroom use is granted without fee provided that copies are not made or distributed for profit or commercial advantage and that copies bear this notice and the full citation on the first page. Copyrights for components of this work owned by others than ACM must be honored. Abstracting with credit is permitted. To copy otherwise, or republish, to post on servers or to redistribute to lists, requires prior specific permission and/or a fee. Request permissions from [permissions@acm.org](mailto:permissions@acm.org).

GECCO '23, July 15–19, 2023, Lisbon, Portugal

© 2023 Association for Computing Machinery.

ACM ISBN 979-8-4007-0119-1/23/07...\$15.00

<https://doi.org/10.1145/3583131.3590407>

of applications involve discrete spaces, such as drug discovery or image generation. Exploring those spaces is challenging as they are combinatorially large and gradients cannot be used in the same manner as in continuous spaces. We introduce MAP-ELITES with a Gradient-Informed Discrete Emitter (ME-GIDE), which extends QD optimisation with differentiable functions over discrete search spaces. ME-GIDE leverages the gradient information of the objective and descriptor functions with respect to its discrete inputs to propose gradient-informed updates that guide the search towards a diverse set of high quality solutions. We evaluate our method on challenging benchmarks including protein design and discrete latent space illumination and find that our method outperforms state-of-the-art QD algorithms in all benchmarks.

## ACM Reference Format:

Raphaël Boige, Guillaume Richard, Jérémie Donà, Antoine Cully, and Thomas Pierrot. 2023. Gradient-Informed Quality Diversity for the Illumination of

Discrete Spaces. In *Proceedings of The Genetic and Evolutionary Computation Conference 2023 (GECCO '23)*. ACM, New York, NY, USA, 14 pages. <https://doi.org/10.1145/3583131.3590407>

## 1 INTRODUCTION

Quality-Diversity (QD) Optimization algorithms [7, 10] have changed the classical paradigm of optimization: inspired by natural evolution, the essence of QD methods is to provide a large and diverse set of high-performing solutions rather than only the best one. This core idea showed great outcomes in different fields such as robotics [9] where it allows to learn to control robots using diverse and efficient policies or latent space exploration [16] of generative models to generate a diverse set of high quality images or video game levels. The main QD approaches are derivative-free optimizers, such as the MAP-ELITES algorithm [40], a genetic algorithm that tries to find high quality solutions covering the space defined by a variety of user-defined features of interest. However, subsequent methods [15, 43] have shown that when the objective functions (quality) or the descriptor functions (diversity) are differentiable, using gradients of those functions can improve convergence both in terms of speed and performance compared to traditional QD algorithms. Those methods were applied to Reinforcement Learning problems such as robotics [47] or latent space illumination [15] of generative adversarial networks.

Those applications focused on optimization over continuous variables. However many real-world applications are best framed using discrete features. For instance, generative architecture such as discrete VAEs [56]; [53] have shown capability to generate high-quality images [50] and have been at the core of recent successful approaches for text-to-image generation [49]; [18]. A further natural application using discrete variables is protein design [27]: proteins play a role in key functions in nature and protein design allows to create new drugs or biofuels. As proteins are sequences of 20 possible amino acids, designing them is a tremendously hard task as only a few of those possible sequences are plausible in the real world. Deep learning for biological sequences provided significant advances in several essential tasks for biological sequence, such as AlphaFold for structure prediction [30] or language models for amino acid likelihood prediction [52]. These successes motivate the use of these tools as objective functions for protein design [2].

In practice, objective functions are often written as differentiable functions of their inputs, enabling the use of gradient information of the continuous extension if the input are discrete [21]. We second this research trend and address gradient informed quality-diversity optimization over discrete inputs when objective and descriptors functions are differentiable. We make several contributions: (i) we introduce MAP-Elites with a Gradient-Informed Discrete Emitter (ME-GIDE), a genetic algorithm where mutations are sampled thanks to a gradient informed distribution. (ii) We propose a way to select the hyperparameters of this algorithm by weighting the importance we give to this gradient information. (iii) We demonstrate the ability of our method to better illuminate discrete spaces on proteins and the discrete latent space of a generative model.

## 2 PROBLEM DEFINITION

In this work, we consider the problem of Quality Diversity Optimization over discrete spaces. The QD problem assumes an objective function  $f : \mathcal{X} \rightarrow \mathbb{R}$ , where  $\mathcal{X}$  is called search space, and  $d$  descriptors  $c_i : \mathcal{X} \rightarrow \mathbb{R}$ , or as a single descriptor function  $\mathbf{c} : \mathcal{X} \rightarrow \mathbb{R}^d$ . We note  $S = \mathbf{c}(\mathcal{X})$  the descriptor space formed by the range of  $\mathbf{c}$ . We only consider discrete spaces of dimension  $m$  with  $K$  categories such that  $\mathcal{X} \subset \{1, \dots, K\}^m$ . QD algorithms of the family of the MAP-ELITES algorithm, discretize the descriptor space  $S$  via a tessellation method. Let  $\mathcal{T}$  be the tessellation of  $S$  into  $M$  cells  $S_i$ . The goal of QD methods is to find a set of solutions  $\mathbf{x}_i \in \mathcal{X}$  so that each solution  $\mathbf{x}_i$  occupies a different cell  $S_i$  in  $\mathcal{T}$  and maximizes the objective function within that cell. The QD objective can thus be formalized as follows:

$$\text{QD-Score} = \max_{\mathbf{x} \in \mathcal{X}} \sum_{i=1}^M f(\mathbf{x}_i), \text{ where } \forall i, \mathbf{c}(\mathbf{x}_i) \in S_i. \quad (1)$$

We consider here that both the objective and descriptor functions are actually defined on real values  $\mathbb{R}$  and restricted to the discrete inputs  $\mathcal{X}$ . We also consider them to be first-order differentiable, hence for any input  $x \in \mathcal{X}$ , we can compute gradients  $\nabla_x f(x)$  and  $\nabla_x c_i(x)$ .

## 3 MAP-ELITES WITH GRADIENT PROPOSAL EMITTER

---

### Algorithm 1: Gradient Informed Discrete Emitter (GIDE)

---

**Given:** a batch of  $B$  elements  $x_n$  from the repertoire and their associated gradients  $\nabla_n$ .

**for**  $1 \leq n \leq B$  **do**

- // Compute the distribution*
- Compute  $\tilde{\delta}_n$  using Equation 3.
- Compute the proposal distribution  $p_n$  using Equation 5.
- // Target entropy*
- Adjust  $T$  to obtain a target entropy  $\bar{H} = \bar{H}_{\text{target}}$  over the proposal distributions.
- // Sample*
- Draw a mutant  $x'_n$  from each  $x_n$  according to  $p_n$ .

**end**

Return  $x'_1, \dots, x'_B$

---

### 3.1 MAP-Elites and Differentiable MAP-Elites

MAP-ELITES is a QD method that discretizes the space of possible descriptors into a repertoire (also called an archive) via a tessellation method. Its goal is to fill each cell of this repertoire with the highest performing individuals. To do so, MAP-ELITES first initializes a repertoire over the BD space and second initializes random solutions, evaluates them and inserts them in the repertoire. Then successive iterations are performed: (i) select and copy solutions uniformly over the repertoire (ii) mutate the copies to create new solution candidates (iii) evaluate the candidates to determine their

descriptor and objective value (iv) find the corresponding cells in the tessellation (v) if the cell is empty, introduce the candidate and otherwise replace the solution already in the cell by the new candidate if it has a greater objective function value. When using real variables, the most popular choice for the mutation operator is the Iso+LineDD [58] that mixes two Gaussian perturbations. When using discrete variables, mutations are generally defined as point mutation, *ie* select a random position and flip its value from the current one to a new one.

To incorporate gradients into MAP-ELITES algorithms, [15] introduced MAP-Elites with a Gradient Arborecence (MEGA) a novel way to use gradient information to guide the mutations. First, the authors propose a novel objective function to encompass both quality and diversity:  $g(x) = |w_0|f(x) + \sum_{i=1}^d w_i c_i(x)$ , where  $w_i \sim \mathcal{N}(0, \sigma_g I) \forall i \in \{0, \dots, d\}$ . In one version of their algorithm, OMG-MEGA, authors simply extend MAP-ELITES by mutating selected element of the repertoires  $x$  via  $x' = x + \nabla_x g(x)$  where  $w_i$  are sampled at each iteration and for each element in the batch and  $\sigma_g$  acts similarly to a learning rate. Indeed, maximizing  $g$  will direct the mutations towards higher fitness and different directions of the descriptor space thanks to the randomness introduced by sampling the  $w_i$ .

### 3.2 From Gradients to the Gradient Informed Discrete Emitter

As this approach has proven effective on several tasks, we follow the previous formulation by trying to maximize  $g$ . In this case at a given iteration, for a given sampled  $x \in \mathcal{X}$  and given sampled coefficients  $c_0, \dots, c_d$ , our emitter should ideally find a neighbour  $x' \in \mathcal{X}$  that maximizes the following:

$$x' = \arg \max_{z \in \mathcal{B}_\tau(x)} \delta(z) = g(z) - g(x) \quad (2)$$

where  $\mathcal{B}_\tau(x)$  is the Hamming ball of size  $\tau$  around  $x$ .

However, for a given variable  $x \in \{1, \dots, K\}^m$ , even for  $\tau = 1$  the cardinality of this Hamming ball is  $mK - 1$ . Hence finding the optimal  $x'$  requires  $mK - 1$  evaluations of  $g$ . Doing it at each step would be too expensive but since those differences are local, they can be approximated using gradient information. Following [21] we use Taylor-series approximation to estimate the local differences at first-order:

$$\delta_{ik} = g(x^{(i,k)}) - g(x) \approx \nabla_x g(x)_{ik} - x_i^T \nabla_x g(x)_i = \tilde{\delta}_{ik} \quad (3)$$

where  $x^{(i,k)}$  differs from  $x$  by a flip on position  $1 \leq i \leq m$  from the current value of  $x_i$  to  $k \in \{1, \dots, K\}$ . The previous formulation works in the case where  $\tau = 1$  but similar approximations can be derived for larger window sizes at the expense of the approximation's quality.

Using those approximations, we could straightforwardly compute a local maximum of  $g$  by taking the argmax of  $\tilde{\delta}_{ik}$  at each step. In order to encourage exploration, we use those approximate local differences to create a proposal distribution over the neighbours of  $x$ . We second traditional sampling technics such as Metropolis Hastings and define the flip distribution  $P$  defined by the probability  $p(x^{(i,k)}|x)$  of mutating from  $x$  to  $x^{(i,k)}$  as

$$p(x^{(i,k)}|x) \propto e^{\frac{\tilde{\delta}_{ik}}{T}} \quad (4)$$

---

#### Algorithm 2: MAP-Elites with Gradient Informed Discrete Emitter (ME-GIDE)

---

**Given:** the number of cells  $M$  and tessellation  $\mathcal{T}$ ; the batch size  $B$  and the number of iterations  $N$ ; the descriptors function  $c$  and the multi-objective function  $f$ ; a target entropy value  $H_{\text{target}}$ ; the initial population of solution candidates  $\{x_k\}$

```

// Initialization
For each initial solution, find the cell corresponding to its descriptor
and add initial solutions to their cells.

// Main loop
for 1 ≤ n_steps ≤ N do
    // Select new generation
    Sample uniformly B solutions x_n in the repertoire with
    replacement

    // Compute the gradients
    Randomly draw weights w^(n) ~ N(0, I)
    Compute gradients ∇_{x_n} f(x_n) and ∇_{x_n} c(x_n)
    Normalize the gradients.
    Compute combined updates
    ∇_n = |w_0^(n)| ∇_{x_n} f(x_n) + ∑_{i=1}^n w_i^(n) ∇_{x_n} c_i(x_n)

    // Gradient-Informed Discrete Emitter
    Use Algorithm 1 to sample mutants x'_n

    // Addition in the archive
    Add each mutant in its corresponding cell if it improves the cell
    fitness, otherwise discard it.
end

```

---

where  $T > 0$  is a temperature parameter. Finally, in order to sample flips at position  $i$  from  $x_i$  to  $k$ , we normalize those probabilities by computing a softmax over every possible flip ( $mK$  possibilities):

$$p(x^{(i,k)}|x) = \frac{e^{\tilde{\delta}_{ik}/T}}{\sum_{j,l=1}^{mK} e^{\tilde{\delta}_{jl}/T}} \quad (5)$$

As every approximated difference  $\tilde{\delta}_{ik}$  can be computed in a single gradient evaluation  $\nabla_x g(x)$ , those probabilities can be efficiently computed. Formally, our Gradient Informed Discrete Emitter (GIDE) receives a candidate  $x$ , computes  $\tilde{\delta}_{ik}$  using Equation 3, then computes mutation probabilities using Equation 5 and finally samples a mutated  $x^{(i,k)}$  using these probabilities. We summarize this procedure in Algorithm 1. Using this emitter, we design our main algorithm: MAP-Elites with a Gradient Informed Discrete Emitter (ME-GIDE). The general procedure follows the one of OMG-MEGA: we first initialize a repertoire of behaviour descriptors. Then at each iteration, the following operations are performed: (i) select a batch of solutions uniformly over the repertoire (ii) sample mutants using our GIDE (iii) evaluate the candidates and add them in the repertoire if their fitness is higher than the existing solution in the cell. This procedure is described in Algorithm 5 with an additional step to control the strength of the gradient guidance defined in the following paragraph.

### 3.3 Controlling the Gradient Guidance with a Target Entropy

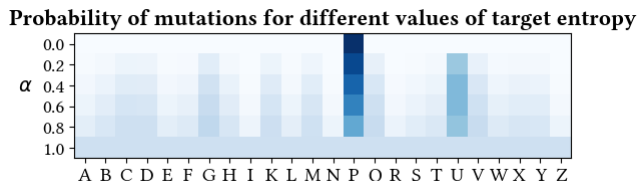


**Figure 2: Probability of mutation for one position in a protein sequence, with the temperature parameter being controlled by the target entropy parametrized as  $H_{target} = \alpha H_{max}$ . Higher target entropy values are associated with smoother flip probabilities.**

The temperature parameter  $T$  controls the shape of the flip distribution  $P_{\tilde{\delta}}$ , as it tempers the softmax operator applied over the estimates  $\tilde{\delta}_{ik}$  according to Equation 4. Tuning this temperature parameter boils down to choosing whether we prefer to greedily follow the highest-gradient direction ( $T \rightarrow 0$ ) or to sample at random a flip direction ( $T \rightarrow \infty$ ). We propose to frame this problem as an exploration-exploitation trade-off, where we suggest to find an optimal temperature parameter  $T = T^*$  such that (1) enough importance is given to the most promising directions, i.e.  $T$  is not too large (2) the improvement-direction estimate is sufficiently peaky to differ from a uniform distribution, i.e.  $T$  is not too small. However, this optimal temperature parameter value  $T$  depends on the dimension of the search space, thus requiring a careful parameter tuning for each domain. Additionally, it also depends on the gradient landscape of the scoring and descriptors functions, which removes any guarantee that a constant value of  $T$  could be optimal throughout the optimization process.

To ease the search of the numerical value of  $T$ , we propose to dynamically adjust it so that the flip distribution matches, in average, a given target Shannon entropy value  $H_{target}$ . Given that we know the analytical form of the flip probability distribution  $P$  thanks to Equation 5, we can express the Shannon entropy as a function of the temperature.

$$H(P) = - \sum_{i,k=1}^{m,K} p(x^{(i,k)}|x) \log(p(x^{(i,k)}|x)) = h(T) \quad (6)$$

For a given entropy target  $H_{target}$  we can solve the equation  $h(T) = H_{target}$  for the value of  $T$ , and dynamically adjust it during the optimization process. The intuition behind using a Shannon entropy target to parametrize the tempered-softmax distribution over  $\tilde{\delta}_{ik}$  is to provide a more interpretable and consistent way to control the exploration-exploitation trade-off, by linking the temperature parameter to a measure of the randomness or uncertainty of the system. Similar Shannon entropy constraints have been previously used in the Reinforcement Learning literature [23].

In practice, at each GIDE update, we use a numerical first-order solver to update the value of the temperature parameter  $T$ , so that we ensure the entropy target is always matched on average. In Figure 2, we illustrate how setting the value of  $H_{target}$  affects the

proposal distribution for the same candidate. As the entropy is bounded by  $[0, H_{max}]$  with  $H_{max} = \log(mk)$ , this allows GIDE to be parameterized by a single hyper-parameter  $\alpha \in [0, 1]$  and to set  $H_{target} = \alpha H_{max}$ .

## 4 EXPERIMENTS

### 4.1 Settings

We conduct experiments on different benchmarks to assess the performance of ME-GIDE. Namely, we experiment on three challenging applications: illuminating a family of proteins, generating diverse digits images by searching a binary pixel space and illuminating the discrete latent space of a generative model. We summarize domain characteristics in Table 1.

*Design in the Ras Protein Family.* As proteins are involved in numerous biological phenomena, including every task of cellular life, designing them has been a longstanding issue for biologists. Relying exclusively on wet-lab experiments to iteratively select designs is both costly and time-consuming so practitioners have turned to in-silico design as a preliminary step. The simplest way to describe a protein is through its primary structure: a natural protein is a sequence of 20 basic chemical elements called amino-acids. Designing a protein is generally framed as finding the sequence of amino acids that maximizes a score representing a property of a protein, such as its ability of binding to a virus or its stability. It is a tedious task as the search space grows exponentially with the length of the protein of interest, for instance designing a protein of 100 residues operates over a space of  $20^{100}$  elements. In our experiment, we aim to redesign members of the ‘‘Rat sarcoma virus’’ (*Ras*) protein family (extracted from PFAM database [38]), involved in cellular signal transduction and playing a role in cancer development [4]. We follow a common objective in computational protein design [27], that focuses on maximizing the stability of a family of protein. While many methods use biophysical simulations to estimate this stability [12], we follow recent trends [1] and use a pre-trained neural network to approximate it. It is worth noting that other works use neural networks and gradient ascent to design proteins but rely on a continuous approximation of proteins [5].

For a given sequence, our objective function is defined as a proxy of the log-likelihood provided by a pre-trained protein language model: ESM2 [36, 52]. Indeed, the log-likelihood has been shown to strongly correlate with the stability of a protein and can even be used to predict the effect of these mutations [25, 51]. We use an unsupervised procedure to create descriptors similar to AURORA [22]: we sample 1,000,000 proteins from the Uniref50<sup>1</sup> database, compute their 640-dimensional embeddings using ESM2 at the 20<sup>th</sup> layer and perform a PCA on those embeddings to extract 5 components. Finally we use a  $K$ -Means algorithm with  $K = 30000$  on these projected embeddings to create the tessellation with 30,000 cells. The descriptors of a sequence is the corresponding projected embedding of this sequence and is mapped to its corresponding cell by finding the closest centroid. In practice, we use the 120,000 elements of this family at initialization.

<sup>1</sup><https://www.uniprot.org/help/uniref>

	Ras protein family	Binarized digits	Discrete LSI - 1	Discrete LSI - 2
<b>Genotype</b>	A protein sequence of length 184	A binary image of dimension $28 \times 28$	A latent code of length 1024	A latent code of length 1024
<b>Search space</b>	$\{0, \dots, 20\}^{184}$	$\{0, 1\}^{28 \times 28}$	$\{0, \dots, 512\}^{1024}$	$\{0, \dots, 512\}^{1024}$
<b>Score</b>	Protein sequence likelihood given by an ESM2 model	Image likelihood given by a RBM model	CLIP similarity score with the prompt: “a labrador”	CLIP similarity score with the prompt: “a truck”
<b>Descriptors</b>	PCA-projected embeddings of ESM2 hidden layer ( $d = 5$ )	PCA-projected embeddings of RBM hidden layer ( $d = 20$ )	CLIP scores with prompts: “a dog with long hair”, “a white puppy” ( $d = 2$ )	CLIP scores with prompts: “a blue truck”, “a red truck” ( $d = 2$ )
<b>Centroids</b>	K-Means centroids (30000 cells)	K-Means centroids (10000 cells)	Voronoi tessellation (30000 cells)	Voronoi tessellation (30000 cells)

Table 1: Experimental setup for each domain: search space, scoring functions, descriptors functions and repertoire used.

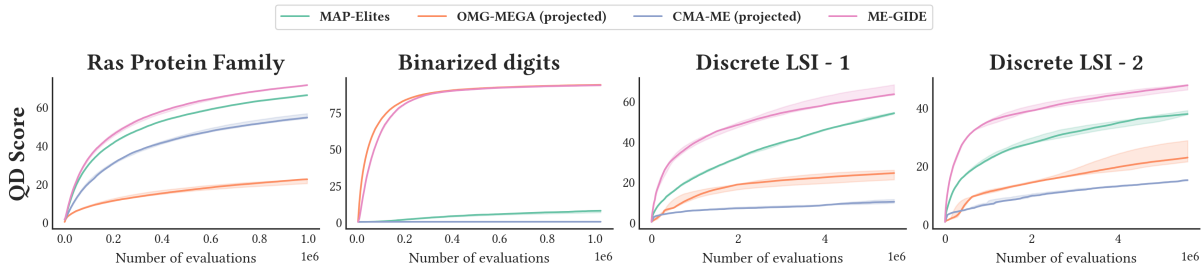


Figure 3: QD-score evolution on the different domains (median and interquartile range over five seeds). ME-GIDE outperforms MAP-ELITES and CMA-MAP-ELITES on every experiment and OMG-MEGA on every experiment except for Binarized Digits. Only the solution corresponding to the best set of hyperparameters are shown for all methods.

*Binarized Digits.* To further illustrate the interest of our method, we design an experiment on binary data consisting in generating diverse MNIST digits with QD methods. Given our fitness and descriptor functions, we aim to find out how QD methods compare in generating diverse digits by directly searching over the image space. We define the fitness using an energy-based model trained on MNIST data. Following [21], we train a restricted Boltzmann machine (RBM) [24] on the binarized  $28 \times 28$  images, we refer the reader to the Appendix A for further details. To obtain descriptors we define a diversity space by embedding the MNIST dataset into the hidden layer of the RBM and then by computing a PCA over these embeddings. Finally, descriptors are defined as projections over the top- $d$  components of this PCA with  $d = 20$ . To compute the centroids, we again use a  $K$ -Means algorithm with  $K = 10000$  on the projected embeddings. We display in Appendix D how this descriptor space spans the different digits’ classes. In our experiments, we initialize our images with uniformly-distributed images from the  $28 \times 28$  binary-images space.

*Discrete Latent Space Illumination (LSI).* Recent works [16], [15] have proposed the latent space illumination of generative models (LSI) problem as a benchmark for QD methods. It consists in searching the latent space of a large generative model for latent codes that can generate diverse images. We follow the setting of [15] using as generative model a discrete latent space VAE instead of a Style-Gan. Since our work is focused on discrete variables, we choose

to illuminate the latent space of a discrete VAE instead of a Style-GAN. Specifically, we selected a vector-quantized auto-encoder (VQ-VAE). We followed the recommendations of the seminal paper [56] to design and train the VQ-VAE on ImageNet [11] data: we use 3 convolutional layers for the encoder and 3 layers for the decoder, a latent vector of size  $32 \times 32 = 1024$  and a codebook size of 512. Thus, each genotype for this experiment is a code of length 1024 from the VQ-VAE latent space, that can take 512 values, resulting in a search space of size  $512^{1024}$ . We refer the reader to the Appendix C for the VQ-VAE model’s details, and the training procedure.

We evaluate the solutions by decoding the proposed discrete latent codes using the pretrained VQ-VAE. We follow previous works in using the CLIP score to measure the similarity between the image and a given prompt. Specifically, we compute one CLIP score for the fitness of the solution and two CLIP scores for the descriptors. We have experimented two settings, composed of two independent sets of prompts. The first one aims to generate labrador images, the fitness is defined with the prompt “A labrador” while the descriptor functions are defined as “A white puppy” and “A dog with long hair”. The second set of prompt searches for truck images, the fitness prompt is “A truck” and descriptor prompts are “A red truck”, “A blue truck”. Further experiment details were deferred to Appendix A. After they are evaluated, solutions are inserted into a CVT [57] repertoire with 30,000 cells. In all our experiments, latent codes were initialized from a random uniform distribution.

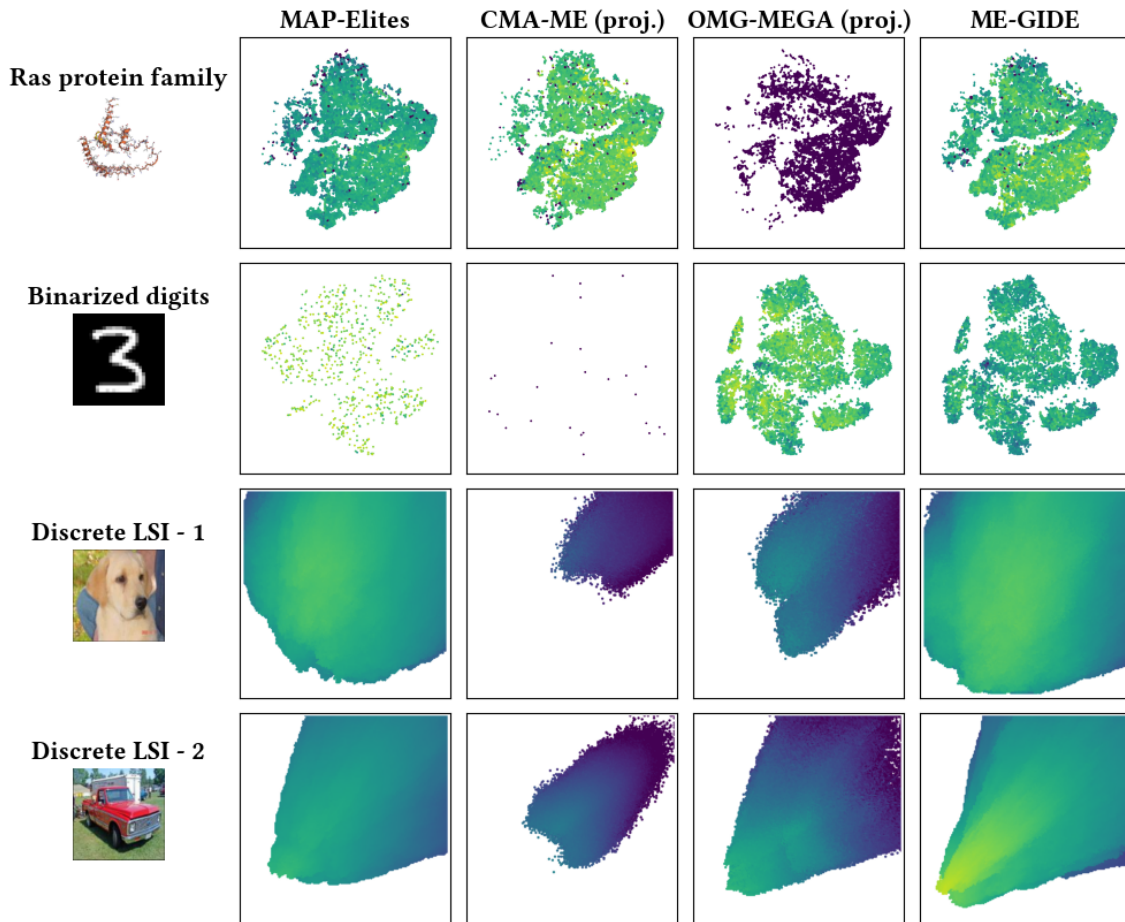


**Figure 4: Repertoires for each domain (line) and method (column). The repertoires of the protein domain (resp. binarized digits domain) have been projected using t-SNE as the original one is 5-dimensional (resp. 20-dimensional). Each point in the repertoire corresponds to a solution, where dark blue corresponds to a low fitness and yellow to a high one.**

*Experiment Setup.* In addition to our ME-GIDE algorithm, we compare with three main baselines. The first baseline, MAP-ELITES stands for the original MAP-ELITES algorithm with completely random one-point mutations: at each step, for each sample solution, the sequence is modified at one position to a uniformly sampled possible value. Searching via random mutations is the most popular solution when no prior knowledge is assumed over the structure of a solution. The second gradient-free baseline is MAP-Elites with Covariance Matrix Adaptation (CMA-MAP-ELITES) [16], an extension of MAP-ELITES that uses CMA as a natural approximation for the gradient and has been shown competitive on many QD tasks. Since CMA-MAP-ELITES has been designed for optimization over continuous spaces, we project back the yielded solutions to the closest points in the discrete space, we hence call this baseline CMA-MAP-ELITES (PROJ.). Finally, our third baseline OMG-MEGA (PROJ.) uses the same projection mechanism applied on the gradient-based method Objective and Measure Gradient MAP-Elites via Gradient Arborecence (OMG-MEGA). The use of this baseline is natural since OMG-MEGA can be considered as the continuous counterpart of ME-GIDE. We give pseudo-codes

for all baselines in Appendix F. It is worth noting that we base our approach on OMG-MEGA rather than CMA-MEGA, the main algorithm proposed for Differentiable Quality Diversity [15] as on our benchmarks, CMA-MEGA was under-performing compared to OMG-MEGA. This can be explained by the fact that CMA updates are based on smoothness assumptions of the gradient that is broken by the projection step to keep solution in the discrete space. We implement our method based on the Jax framework and use the QDax open source library [6, 34] for the baselines.

We run every experiment over five different seeds for each method. Note that in the protein experiment, all methods are combined with crossover where half of the sampled solutions are modified with the method-specific emitter and the other half with crossover. We stop the illumination after evaluating 1,000,000 candidates on the protein and binarized digits experiment and 5,000,000 evaluations for the discrete LSI experiments. We provide more details about the settings in Appendix A.

## 4.2 Results and Analysis

*Performance Analysis.* Figure 3 summarizes the results of our experiments: we display the median QD score and the interquartile range over the five random seeds for every benchmark. In the Ras and Discrete LSI experiments, ME-GIDE outperforms other methods, since it converges in fewer iterations to higher performances. We use a Wilcoxon signed-rank test [59] to compare the distribution of the scores obtained over different seeds where the null hypothesis is that the obtained scores have the same median. It shows that ME-GIDE constantly outperforms MAP-ELITES and CMA-MAP-ELITES (PROJ.) in the QD score with p-values lower than 0.05 in every experiment and outperforms OMG-MEGA (PROJ.) on every experiment except Binarized Digits.

*Entropy ablations.* For clarity, we only plot the results corresponding for the best set of hyperparameters for each baseline, although we ran a hyperparameter search for each method with comparable budget as detailed in Appendix A. Our target entropy procedure allows an easier choice of hyperparameters for ME-GIDE as we only need to choose  $\alpha$  within a natural range  $[0, 1]$ . In our experiment, we try for four values for  $\alpha \in \{0.2, 0.4, 0.6, 0.8\}$ , we don't test  $\alpha = 1$  as it corresponds to standard MAP-ELITES with random uniform mutations. While we display the results for the best value of  $\alpha$  in Figure 3, the conclusions are similar for other values of  $\alpha$  as detailed in Appendix B.

*Difficulty of gradient-informed optimization.* Interestingly, OMG-MEGA under-performs compared to purely random mutations for any set of hyperparameters on both protein and Discrete LSI experiments. This means performing gradient descent similarly as in the continuous case is perilous when using discrete variables as it will likely yield unfeasible solutions with no guarantee that the closest feasible point is a viable solution. As stated in Section 3, our method relies on the fact that our gradient approximation  $\tilde{\delta}$  is a good surrogate for the true improvement  $\delta(x') = g(x') - g(x)$ . This approximation relies on a smoothness assumption of those functions and the fact that neighbours stay "close" in the continuous space. We validate this assumption via the following procedure: (i) randomly sample some points  $x_i$  (ii) compute for each of their neighbour  $x'_i$  both  $\delta(x'_i)$  and  $\tilde{\delta}(x'_i)$  ( $\tilde{\delta}$  only needs to be computed once) and (iii) compute the correlation  $\rho_{\tilde{\delta}}(x)$  between those two quantities. For instance, we display the distribution of correlations for 1,000 elements for the Discrete LSI-1 experiment in Figure 5, where we find an average correlation  $\rho = 0.59$ , which means that even though the step between  $x^{(i,k)}$  and  $x$  might be large, gradient information is indeed relevant.

*Qualitative analysis.* We display some proteins of the final repertoire obtained by ME-GIDE in Figure 6. To visualize the 3D structure of those proteins, we use AlphaFold2 [29]. One can qualitatively see that ME-GIDE manages to extract proteins with various secondary and tertiary structures and that those proteins have high confidence score according to AlphaFold. We also conduct further quantitative validation on the protein experiment of our method ME-GIDE against MAP-ELITES which is the best alternative baseline in this experiment. We sub-sample our repertoire by recomputing larger cells to obtain a repertoire with 300 cells. Then, we insert the original repertoire into this smaller one to obtain the most fit solutions

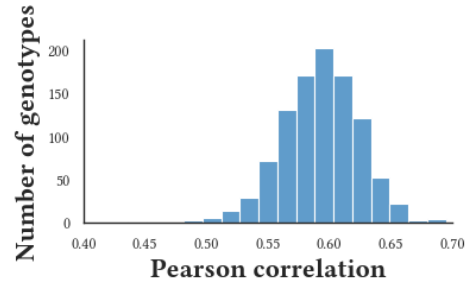


**Figure 5: Pearson correlation between the true improvement  $\delta(x') = g'(x) - g(x)$  and GIDE estimate  $\tilde{\delta}(x')$ . We sampled 1000 random latent codes from the *Discrete LSI - 1* domain, we evaluated the true improvement by enumerating all the possible neighbors and we computed the correlation with the GIDE estimate. We display the distribution of these correlations across the 1000 different latent codes.**

in each region. We first analyze the diversity in the sequence space, defined as the average edit distance between obtained solutions. We find that ME-GIDE reaches an average distance of 106.9 whereas MAP-ELITES gets 97.2. We also use *S4Pred* [39] to predict the secondary structure of each protein and use the average edit distance between secondary structures. ME-GIDE outperforms MAP-ELITES, obtaining an average distance of 44.2 against 34.9, and finds more diverse structures while also reaching an overall higher average fitness.

In Figure 6, we also display some samples found by ME-GIDE on the binarized MNIST experiment. One can see that ME-GIDE is able to find diverse images that resemble MNIST images and covers every digit. We also visualize top-performing images from the repertoire learned by ME-GIDE as well as natural images from the ImageNet dataset. Images found by ME-GIDE cannot be considered to match the prompt from a human point of view although a small shape of a dog appears in the center of the image. It should still be noted that these images have higher CLIP scores than natural images that humans would score as perfectly aligned with the score prompt. In a sense, we corroborate previous findings, such as [41], proving that neural networks classifiers are easily fooled by evolutionary algorithms or gradient based attacks. Our study highlights the difficulty of directly sampling relevant latent codes in the latent space of a discrete VAE, which is in general bypassed by an additional auto-regressive model that learns to sample meaningful latent codes.

## 5 RELATED WORKS

*Discrete Optimization.* Discrete optimization [46] is a longstanding branch of optimization where some of the variables or constraints are discrete. It is also named combinatorial optimization as the set of feasible solutions is generally finite but evaluation every solution is irrealizable. A first class of algorithms search for an exact solution: in particular, Integer Linear Programming [54] has been the main subject of interest with exact methods such as cutting plan [19] or branch and bound [31]. On the other hand, evolutionary algorithms have been very popular as they allow for

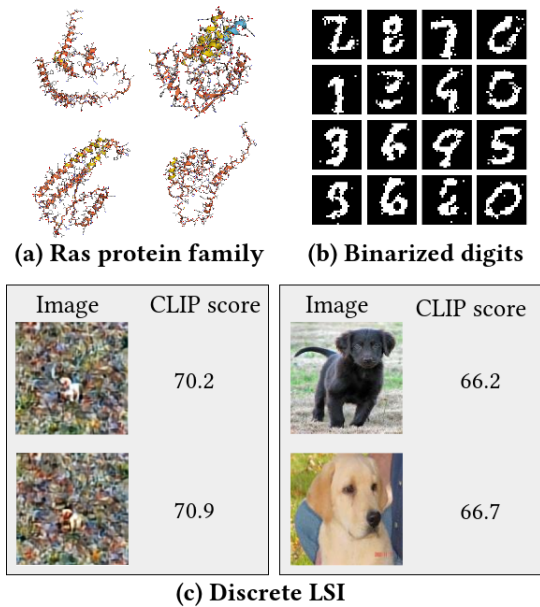


**Figure 6: Illustration of the obtained solutions on the 3 domains. (a) Ras proteins designed by ME-GIDE, visualized using the prediction of AlphaFold. One can see diverse patterns in the secondary structure, while still retaining high estimated stability. (b) Samples from ME-GIDE final repertoire on the Binarized Digits experiment. We downsample the 10,000 elements in the repertoire by clustering its centroids to 16 to re-create a repertoire with 16 cells, projecting the obtained images in the downsampled repertoire. (c) Samples found by ME-GIDE on the "Labrador" prompt against highest scoring images from ImageNet dataset. While the images found by ME-GIDE are not natural images, they achieve a higher score to be a "labrador" according to CLIP.**

more flexibility and can be stopped at any iteration to get the best solution explored so far [13]. Most of those algorithms either incorporate this knowledge by mutating only to feasible solutions or use a relaxation and then project back to the feasible set [35]. For instance, for protein design, exact methods have been proposed for specific biophysical cost functions related to the potential energy [12] of the protein or its binding affinity [45]. However, due to the limitations in flexibility of the previous methods, the most popular design tool, incorporated in the popular *Rosetta* library, is based on simulated annealing [26]. Several work tried to leverage recent breakthroughs of deep learning methods tailored to proteins in the protein design, such as *AlphaDesign* [28] or *TrDesign* [44]. Other works have proposed gradient-based methods for biological sequence design: some work run gradient ascent on a continuous one-hot representation [37]; others train an auto-encoder alongside the scoring function and feed the latent representation as input to the latter while gradient is carried out through this latent space [20]. To the best of our knowledge, our work is the first to propose QD as a solution for protein design.

*Quality Diversity Optimization.* Searching for novelty instead of quality [32] was the first work formulating diversity as an end

in itself. It was further refined by introducing a notion of local quality with local competition [33]. MAP-ELITES [40] refined the notion of diversity by introducing the notion of repertoire over a set of descriptors. Further improvement were made on the design the descriptor space such as using a Voronoi tessellation [57] or use unsupervised descriptors [8, 22] as defining tailored descriptors can be tedious for some tasks. More efficient ways to illuminate this space have been proposed, such as more efficient mutation operators [58] or covariance matrix adaptation [17]. Closest to this work is Differentiable QD [15] where gradients are used to directly update over the continuous variables.

Application specific methods were developed to apply QD algorithms to noisy domains [14] or when multiple objectives are at stake [48]. Reinforcement Learning is one of the most popular applications of QD [3] and some methods try to incorporate diversity directly in RL algorithms [43, 47]. QD methods have already been applied to Latent Space Exploration, one of the domains we experiment on. The earliest work was named Innovation Engines [42] where authors try to generate diverse images using a QD approach over ImageNet. Later Latent Space Illumination has been introduced to generate game levels [55] or images [15]. Our work is also applicable to LSI in the case of a discrete latent space and is the first work of its kind to the best of authors' knowledge.

## 6 CONCLUSION

We introduced ME-GIDE, a genetic algorithm that leverages gradient information over discrete variables for Quality Diversity optimization and show it outperforms classical baselines. Our entropy-based guidance allows to ease the search for good hyperparameters which can be tedious for some applications. Our experiment on protein design is the first using QD methods to the best of author's knowledge and this opens a way for more applications in the future. Indeed, we believe that generating not only fit but also diverse proteins can be useful as the fitness given by the model does not always translate to good properties in the lab.

Our goal was not to propose a novel image generation technique but while the results of our LSI experiment are interpretable and ME-GIDE finds images with higher fitnesses than realistic images, further research can be done to better understand and exploit these results. Our method can be used to create adversarial examples for generative models using discrete latent spaces, that are becoming more and more popular. On the other hand, to generate more realistic images, we could constrain the search to a few latent codes and use a recurrent architecture to generate a more realistic prior, at the cost of potentially facing vanishing or exploding gradients. We leave these open questions for future works.

As our method involves computing gradients of the fitness and descriptor functions, we expect it to be intractable for functions involving large neural networks, such as AlphaFold. Using a surrogate model to guide the search while keeping a large model for evaluation or validation to handle those cases could be a promising research direction.

## ACKNOWLEDGEMENT

This work was supported by the Google's TPU Research Cloud (TRC).



## REFERENCES

- [1] Ivan Anishchenko, Samuel J Pellock, Tamuka M Chidyausiku, Theresa A Ramelot, Sergey Ovchinnikov, Jingzhou Hao, Khushboo Bafna, Christoffer Norn, Alex Kang, Asim K Bera, et al. 2021. De novo protein design by deep network hallucination. *Nature* 600, 7889 (2021), 547–552.
- [2] Ivan Anishchenko, Samuel J. Pellock, Tamuka M. Chidyausiku, Theresa A. Ramelot, Sergey Ovchinnikov, Jingzhou Hao, Khushboo Bafna, Christoffer Norn, Alex Kang, Asim K. Bera, Frank DiMaio, Lauren Carter, Cameron M. Chow, Gaetano T. Montelione, and David Baker. 2021. De novo protein design by deep network hallucination. *Nature* 600, 7889 (01 Dec 2021), 547–552. <https://doi.org/10.1038/s41586-021-04184-w>
- [3] Kai Arulkumaran, Antoine Cully, and Julian Togelius. 2019. Alphastar: An evolutionary computation perspective. In *Proceedings of the genetic and evolutionary computation conference companion*. 314–315.
- [4] Johannes L Bos. 1989. Ras oncogenes in human cancer: a review. *Cancer research* 49, 17 (1989), 4682–4689.
- [5] Egbert Castro, Abhinav Godavarthi, Julian Rubinfiem, Kevin Givechian, Dhananjay Bhaskar, and Smita Krishnaswamy. 2022. Transformer-based protein generation with regularized latent space optimization. *Nature Machine Intelligence* 4, 10 (2022), 840–851.
- [6] Felix Chalumeau, Bryan Lim, Raphael Boige, Maxime Allard, Luca Grillotti, Manon Flageat, Valentin Macé, Arthur Flajolet, Thomas Pierrot, and Antoine Cully. 2023. QDax: A Library for Quality-Diversity and Population-based Algorithms with Hardware Acceleration. *arXiv preprint arXiv:2308.03665* (2023).
- [7] Konstantinos Chatzilygeroudis, Antoine Cully, Vassilis Vassiliades, and Jean-Baptiste Mouret. 2021. Quality-Diversity Optimization: a novel branch of stochastic optimization. In *Black Box Optimization, Machine Learning, and No-Free Lunch Theorems*. Springer, 109–135.
- [8] Antoine Cully. 2019. Autonomous skill discovery with quality-diversity and unsupervised descriptors. In *Proceedings of the Genetic and Evolutionary Computation Conference*. 81–89.
- [9] Antoine Cully, Jeff Clune, Danesh Tarapore, and Jean-Baptiste Mouret. 2015. Robots that can adapt like animals. *Nature* 521, 7553 (2015), 503–507.
- [10] Antoine Cully and Yiannis Demiris. 2017. Quality and diversity optimization: A unifying modular framework. *IEEE Transactions on Evolutionary Computation* 22, 2 (2017), 245–259.
- [11] Jia Deng, Wei Dong, Richard Socher, Li-Jia Li, Kai Li, and Li Fei-Fei. 2009. Imagenet: A large-scale hierarchical image database. In *2009 IEEE conference on computer vision and pattern recognition*. Ieee, 248–255.
- [12] Johan Desmet, Marc De Maeyer, Bart Hazes, and Ignace Lasters. 1992. The dead-end elimination theorem and its use in protein side-chain positioning. *Nature* 356, 6369 (1992), 539–542.
- [13] Marco Dorigo, Gianni Di Caro, and Luca M Gambardella. 1999. Ant algorithms for discrete optimization. *Artificial life* 5, 2 (1999), 137–172.
- [14] Manon Flageat and Antoine Cully. 2020. Fast and stable MAP-Elites in noisy domains using deep grids. *arXiv preprint arXiv:2006.14253* (2020).
- [15] Matthew Fontaine and Stefanos Nikolaidis. 2021. Differentiable quality diversity. *Advances in Neural Information Processing Systems* 34 (2021), 10040–10052.
- [16] Matthew C Fontaine, Ruilin Liu, Ahmed Khalifa, Jignesh Modi, Julian Togelius, Amy K Hoover, and Stefanos Nikolaidis. 2021. Illuminating mario scenes in the latent space of a generative adversarial network. In *Proceedings of the AAAI Conference on Artificial Intelligence*, Vol. 35. 5922–5930.
- [17] Matthew C Fontaine, Julian Togelius, Stefanos Nikolaidis, and Amy K Hoover. 2020. Covariance matrix adaptation for the rapid illumination of behavior space. In *Proceedings of the 2020 genetic and evolutionary computation conference*. 94–102.
- [18] Oran Gafni, Adam Polyak, Oron Ashual, Shelly Sheynin, Devi Parikh, and Yaniv Taigman. 2022. Make-a-scene: Scene-based text-to-image generation with human priors. *arXiv preprint arXiv:2203.13131* (2022).
- [19] Paul C Gilmore and Ralph E Gomory. 1961. A linear programming approach to the cutting-stock problem. *Operations research* 9, 6 (1961), 849–859.
- [20] Rafael Gómez-Bombarelli, Jennifer N Wei, David Duvenaud, José Miguel Hernández-Lobato, Benjamin Sánchez-Lengeling, Dennis Sheberla, Jorge Aguilera-Iparraguirre, Timothy D Hirzel, Ryan P Adams, and Alán Aspuru-Guzik. 2018. Automatic chemical design using a data-driven continuous representation of molecules. *ACS central science* 4, 2 (2018), 268–276.
- [21] Will Grathwohl, Kevin Swersky, Milad Hashemi, David Duvenaud, and Chris Maddison. 2021. Oops i took a gradient: Scalable sampling for discrete distributions. In *International Conference on Machine Learning*. PMLR, 3831–3841.
- [22] Luca Grillotti and Antoine Cully. 2022. Unsupervised behaviour discovery with quality-diversity optimisation. *IEEE Transactions on Evolutionary Computation* (2022).
- [23] Tuomas Haarnoja, Aurick Zhou, Kristian Hartikainen, George Tucker, Sehoon Ha, Jie Tan, Vikash Kumar, Henry Zhu, Abhishek Gupta, Pieter Abbeel, et al. 2018. Soft actor-critic algorithms and applications. *arXiv preprint arXiv:1812.05905* (2018).
- [24] Geoffrey E Hinton. 2012. A practical guide to training restricted Boltzmann machines. In *Neural networks: Tricks of the trade*. Springer, 599–619.
- [25] Thomas A Hopf, John B Ingraham, Frank J Poelwijk, Charlotta PI Schärfe, Michael Springer, Chris Sander, and Debora S Marks. 2017. Mutation effects predicted from sequence co-variation. *Nature biotechnology* 35, 2 (2017), 128–135.
- [26] Po-Ssu Huang, Yih-En Andrew Ban, Florian Richter, Ingemar Andre, Robert Vernon, William R Schief, and David Baker. 2011. RosettaRemodel: a generalized framework for flexible backbone protein design. *PLoS one* 6, 8 (2011), e24109.
- [27] Po-Ssu Huang, Scott E Boyken, and David Baker. 2016. The coming of age of de novo protein design. *Nature* 537, 7620 (2016), 320–327.
- [28] Michael Jendrusch, Jan O Korbel, and S Kashif Sadiq. 2021. AlphaDesign: A de novo protein design framework based on AlphaFold. *bioRxiv* (2021).
- [29] John Jumper, Richard Evans, Alexander Pritzel, Tim Green, Michael Figurnov, Olaf Ronneberger, Kathryn Tunyasuvunakool, Russ Bates, Augustin Židek, Anna Potapenko, et al. 2021. Highly accurate protein structure prediction with AlphaFold. *Nature* 596, 7873 (2021), 583–589.
- [30] John Jumper, Richard Evans, Alexander Pritzel, Tim Green, Michael Figurnov, Olaf Ronneberger, Kathryn Tunyasuvunakool, Russ Bates, Augustin Židek, Anna Potapenko, Alex Bridgland, Clemens Meyer, Simon A. A. Kohl, Andrew J. Ballard, Andrew Cowie, Bernardino Romera-Paredes, Stanislaw Nikolov, Rishub Jain, Jonas Adler, Trevor Back, Stig Petersen, David Reiman, Ellen Clancy, Michal Zieliński, Martin Steinegger, Michalina Pacholska, Tamas Berghammer, Sebastian Bodensteiner, David Silver, Oriol Vinyals, Andrew W. Senior, Koray Kavukcuoglu, Pushmeet Kohli, and Demis Hassabis. 2021. Highly accurate protein structure prediction with AlphaFold. *Nature* 596, 7873 (01 Aug 2021), 583–589. <https://doi.org/10.1038/s41586-021-03819-2>
- [31] Ailsa H Land and Alison G Doig. 2010. An automatic method for solving discrete programming problems. In *50 Years of Integer Programming 1958-2008*. Springer, 105–132.
- [32] Joel Lehman and Kenneth O Stanley. 2011. Abandoning objectives: Evolution through the search for novelty alone. *Evolutionary computation* 19, 2 (2011), 189–223.
- [33] Joel Lehman and Kenneth O Stanley. 2011. Evolving a diversity of virtual creatures through novelty search and local competition. In *Proceedings of the 13th annual conference on Genetic and evolutionary computation*. 211–218.
- [34] Bryan Lim, Maxime Allard, Luca Grillotti, and Antoine Cully. 2022. Accelerated Quality-Diversity for Robotics through Massive Parallelism. *arXiv preprint arXiv:2202.01258* (2022).
- [35] C-Y Lin and Prabhat Hajela. 1992. Genetic algorithms in optimization problems with discrete and integer design variables. *Engineering optimization* 19, 4 (1992), 309–327.
- [36] Zeming Lin, Halil Akin, Roshan Rao, Brian Hie, Zhongkai Zhu, Wenting Lu, Allan dos Santos Costa, Maryam Fazel-Zarandi, Tom Sercu, Sal Candido, and Alexander Rives. 2022. Language models of protein sequences at the scale of evolution enable accurate structure prediction. *bioRxiv* (2022). <https://doi.org/10.1101/2022.07.20.500902>
- [37] Ge Liu, Haoyang Zeng, Jonas Mueller, Brandon Carter, Ziheng Wang, Jonas Schilz, Geraldine Horny, Michael E Birnbaum, Stefan Ewert, and David K Gifford. 2020. Antibody complementarity determining region design using high-capacity machine learning. *Bioinformatics* 36, 7 (2020), 2126–2133.
- [38] Jaina Mistry, Sara Chuguransky, Lowri Williams, Matloob Qureshi, Gustavo A Salazar, Erik LL Sonnhammer, Silvio CE Tosatto, Lisanna Paladin, Shriya Raj, Lorna J Richardson, et al. 2021. Pfam: The protein families database in 2021. *Nucleic acids research* 49, D1 (2021), D412–D419.
- [39] Lewis Moffat and David T Jones. 2021. Increasing the accuracy of single sequence prediction methods using a deep semi-supervised learning framework. *Bioinformatics* 37, 21 (2021), 3744–3751.
- [40] Jean-Baptiste Mouret and Jeff Clune. 2015. Illuminating search spaces by mapping elites. *arXiv preprint arXiv:1504.04909*.
- [41] Anh Nguyen, Jason Yosinski, and Jeff Clune. 2015. Deep neural networks are easily fooled: High confidence predictions for unrecognizable images. In *Proceedings of the IEEE conference on computer vision and pattern recognition*. 427–436.
- [42] Anh Mai Nguyen, Jason Yosinski, and Jeff Clune. 2015. Innovation engines: Automated creativity and improved stochastic optimization via deep learning. In *Proceedings of the 2015 Annual Conference on Genetic and Evolutionary Computation*. 959–966.
- [43] Olle Nilsson and Antoine Cully. 2021. Policy gradient assisted map-elites. In *Proceedings of the Genetic and Evolutionary Computation Conference*. 866–875.
- [44] Christoffer Norn, Basile IM Wicky, David Juergens, Sirui Liu, David Kim, Doug Tischer, Brian Koepnick, Ivan Anishchenko, Foldit Players, David Baker, et al. 2021. Protein sequence design by conformational landscape optimization. *Proceedings of the National Academy of Sciences* 118, 11 (2021), e2017228118.
- [45] Adegoke A Ojewole, Jonathan D Jou, Vance G Fowler, and Bruce R Donald. 2018. BBK\*(Branch and Bound Over K\*): A provable and efficient ensemble-based protein design algorithm to optimize stability and binding affinity over large sequence spaces. *Journal of Computational Biology* 25, 7 (2018), 726–739.
- [46] R Gary Parker and Ronald L Rardin. 2014. *Discrete optimization*. Elsevier.
- [47] Thomas Pierrot, Valentin Macé, Felix Chalumeau, Arthur Flajolet, Geoffrey Cideron, Karim Beguir, Antoine Cully, Olivier Sigaud, and Nicolas Perrin-Gilbert.

2022. Diversity Policy Gradient for Sample Efficient Quality-Diversity Optimization. In *ICLR Workshop on Agent Learning in Open-Endedness*.
- [48] Thomas Pierrot, Guillaume Richard, Karim Beguir, and Antoine Cully. 2022. Multi-Objective Quality Diversity Optimization. *arXiv preprint arXiv:2202.03057* (2022).
- [49] Aditya Ramesh, Mikhail Pavlov, Gabriel Goh, Scott Gray, Chelsea Voss, Alec Radford, Mark Chen, and Ilya Sutskever. 2021. Zero-shot text-to-image generation. In *International Conference on Machine Learning*. PMLR, 8821–8831.
- [50] Ali Razavi, Aaron Van den Oord, and Oriol Vinyals. 2019. Generating diverse high-fidelity images with vq-vae-2. *Advances in neural information processing systems* 32 (2019).
- [51] Adam J Riesselman, John B Ingraham, and Debora S Marks. 2018. Deep generative models of genetic variation capture the effects of mutations. *Nature methods* 15, 10 (2018), 816–822.
- [52] Alexander Rives, Joshua Meier, Tom Sercu, Siddharth Goyal, Zeming Lin, Jason Liu, Demi Guo, Myle Ott, C Lawrence Zitnick, Jerry Ma, et al. 2021. Biological structure and function emerge from scaling unsupervised learning to 250 million protein sequences. *Proceedings of the National Academy of Sciences* 118, 15 (2021), e2016239118.
- [53] Jason Tyler Rolfe. 2016. Discrete variational autoencoders. *arXiv preprint arXiv:1609.02200* (2016).
- [54] Alexander Schrijver. 1998. *Theory of linear and integer programming*. John Wiley & Sons.
- [55] Jacob Schrum, Vanessa Volz, and Sebastian Risi. 2020. Cppn2gan: Combining compositional pattern producing networks and gans for large-scale pattern generation. In *Proceedings of the 2020 Genetic and Evolutionary Computation Conference*. 139–147.
- [56] Aaron Van Den Oord, Oriol Vinyals, et al. 2017. Neural discrete representation learning. *Advances in neural information processing systems* 30 (2017).
- [57] Vassilis Vassiliades, Konstantinos Chatzilygeroudis, and Jean-Baptiste Mouret. 2017. Using centroidal voronoi tessellations to scale up the multidimensional archive of phenotypic elites algorithm. *IEEE Transactions on Evolutionary Computation* 22, 4 (2017), 623–630.
- [58] Vassilis Vassiliades and Jean-Baptiste Mouret. 2018. Discovering the elite hypervolume by leveraging interspecies correlation. In *Proceedings of the Genetic and Evolutionary Computation Conference*. 149–156.
- [59] Frank Wilcoxon. 1992. Individual comparisons by ranking methods. In *Breakthroughs in statistics*. Springer, 196–202.

## A EXPERIMENT SETTINGS DETAILS

In this section we provide additional information about the experiments settings.

*Design in the Ras Protein Family.* Input sequences are restricted to a maximum length of 186 with 25 possible amino acids. We use the *esm2\_t30\_150M\_UR50D* architecture from the ESM2 repository<sup>2</sup>, which is made of 30 attention layers and 150 millions of parameters in total. We use the 120,000 elements of the PFAM database to initialize the repertoire in every experiment. We use a batch size of 126 at each iteration and perform 7937 iterations to evaluate 1,000,000 elements in total. Every method is run for a total of five trials. ME-GIDE was run for four values of target entropy: 0.2, 0.4, 0.6 and 0.8. MAP-ELITES was run with different values of number of mutations at each iteration but the best results were obtained with 1–point mutation at each iteration. OMG-MEGA was run for values of  $\sigma_g = 0.1, 1, 10, 100, 1000$  and the best results were obtained for  $\sigma_g = 100$ . CMA-MAP-ELITES was run for values of initial standard deviation of  $\sigma_0 = 0.01, 0.05, 0.1, 0.5, 1.0, 5.0$  and the best results were obtained for  $\sigma_0 = 0.5$

*Binarized digits.* Input images are treated as vectors of length 784 with 2 possibilities (0 or 1). We use a RBM with 500 hidden units and we train it with the contrastive divergence algorithm. We initialize the repertoire uniformly at random. We use a batch size of 512 at each iteration and perform 2000 iterations to evaluate 1,024,000 elements in total. Every method is run for a total of five trials. ME-GIDE was run for four values of target entropy: 0.2, 0.4, 0.6 and 0.8. MAP-ELITES was run with different values of number of mutations at each iteration and with crossover but the best results were obtained with 1–point mutation at each iteration and no crossover. OMG-MEGA (PROJ.) was run for values of  $\sigma_g = 1, 10, 100$  and the best results were obtained for  $\sigma_g = 10$  in value. CMA-MAP-ELITES was run for values of initial standard deviation of  $\sigma_0 = 0.01, 0.05, 0.1, 0.5, 1.0, 5.0$  and the best results were obtained for  $\sigma_0 = 0.5$

*Discrete LSI.* The latent space is made of  $32 \times 32 = 1024$  codes with 512 possibilities. We use a VQ-VAE which architecture is detailed in Appendix C. We initialize the repertoire uniformly at random. We use a batch size of 560 at each iteration and perform 10000 iterations to evaluate 5,600,000 elements in total. Every method is run for a total of five trials. ME-GIDE was run for four values of target entropy: 0.2, 0.4, 0.6 and 0.8. MAP-ELITES was run with different values of number of mutations at each iteration and with crossover but the best results were obtained with 1–point mutation at each iteration and no crossover. OMG-MEGA (PROJ.) was run for values of  $\sigma_g = 1, 10, 100$  and the best results were obtained for  $\sigma_g = 100$ . CMA-MAP-ELITES was run for values of initial standard deviation of  $\sigma_0 = 0.01, 0.05, 0.1, 0.5, 1.0, 5.0$  and the best results were obtained for  $\sigma_0 = 0.5$ . Concerning the descriptors and objective range, the CLIP-based descriptors are scalar values ranging from 0 to 10, lower descriptor indicating stronger similarity. To compute the fitness score, we transform the score associated with the fitness prompt by applying the function  $x \mapsto (10 - x) \times 10$ . Thus we obtain a score ranging from 0 to 100 as displayed in the Figure 6.

<sup>2</sup><https://github.com/facebookresearch/esm>

## B DETAILED RESULTS FOR DIFFERENT TARGET ENTROPIES

In all of our experiments we run our method for four values of entropy and only plot the best one in Figure 3. We show here that for any value of target entropy in  $\{0.2, 0.4, 0.6, 0.8\}$ , ME-GIDE outperforms other baselines on the protein domain and the discrete LSI domains. It highlights the robustness of ME-GIDE regarding the exact choice of entropy target. For the binarized digits domain, a lower target entropy induces faster convergence, this is mainly due to the fact that the dimensions of the problem makes it easier to solve, hence favoring methods that can greedily follow gradient signal.

## C VQ-VAE ARCHITECTURE

To train our VQ-VAE, we follow guidelines of [56]. We train our VQ-VAE on ImageNet<sup>3</sup> where images are pre-processed to be of size  $128 \times 128$ . We use the same architecture as the authors of the aforementioned paper and use a latent vector of size  $32 \times 32 = 1024$  with a codebook size of 512. We use 3 convolutional layers for the encoder and 3 layers for the decoder. We use *Adam* optimizer with a learning rate  $\eta = 2e - 4$  we set the commitment loss coefficient to  $\beta = 0.25$ .

## D VISUALIZATION OF THE MNIST DATA IN THE DESCRIPTOR SPACE

On complex data such as MNIST binary images, it is no easy task to define a relevant descriptor space. To characterize the diversity of different images of digits, one possible solution is to use the features extracted by a Deep Neural Network trained for the classification task. We instead chose to use the features implicitly embedded in the hidden layer of the RBM trained on the MNIST data. As the RBM model is trained for likelihood estimation, we expect it to learn a robust representation of the data, that efficiently separate the different classes of digits. To further validate this choice, we visualize a projection of the MNIST dataset in our embedding space. To do so, we first embed the whole dataset in the 20-dimensional descriptor space, then we project it in dimension 2 using the t-SNE algorithm. In Figure 8 we showcase MNIST images sampled uniformly in the projection space. It demonstrates the fact that our descriptor space properly spread the MNIST different classes and is able to characterize the diversity in the digits' space.

## E VALIDATION ON PROTEIN DATA

We visualize the diversity obtained on proteins with two information: primary structure and secondary structure. First, we sub-sample to 300 the repertoire obtained with MAP-ELITES and ME-GIDE by performing a  $K = 300$ -means clustering on the centroids of the repertoire. Then every protein from the original repertoire is added to the new one, keeping only the most fit in every region. We evaluate diversity in the primary structure (amino acid sequence) by computing the pairwise Levenshtein distances between each protein. We display the histograms of the distributions of pairwise distances betweenw MAP-ELITES and ME-GIDE in Figure 9.

<sup>3</sup><https://www.image-net.org/>

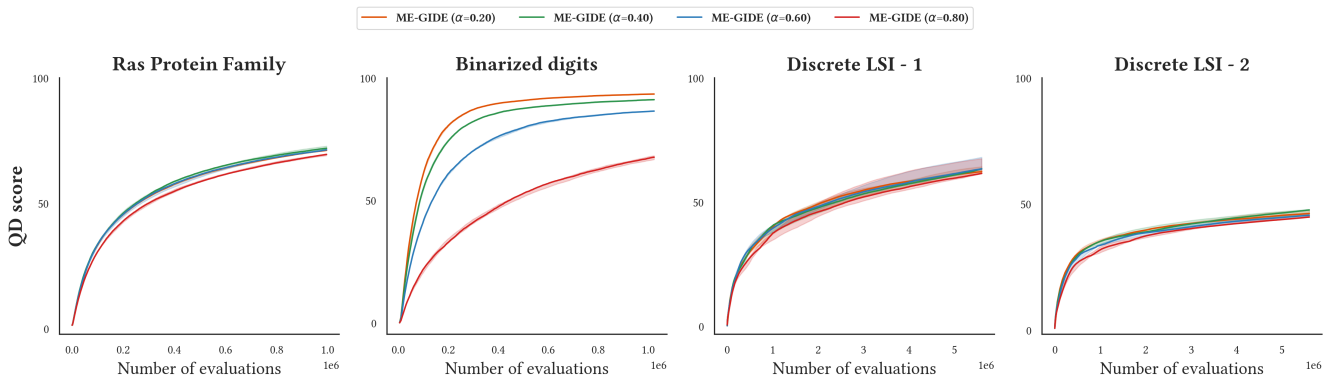


Figure 7: QD-score evolution on the different domains (median and interquartile range over five seeds) for different values of target entropy. On three out of the four domains, different values of target entropy yield similar results. It demonstrates that the use of a target entropy eases the hyperparameter tuning procedure.

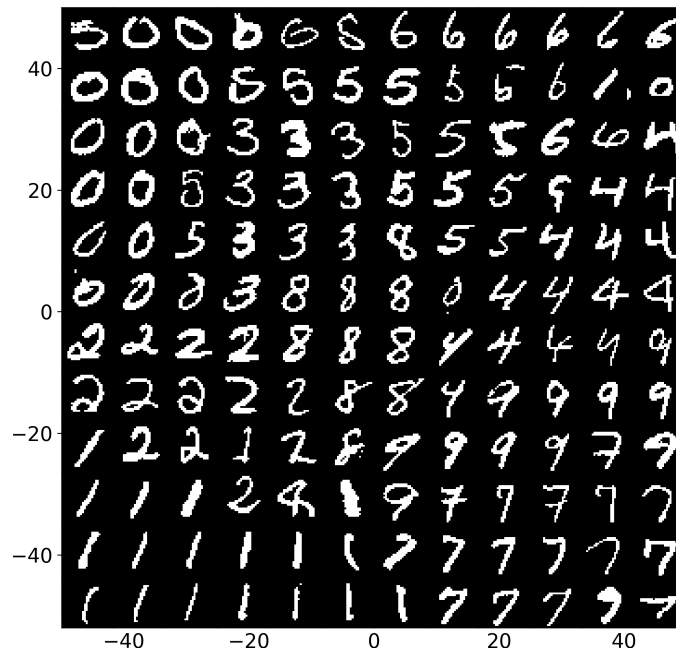
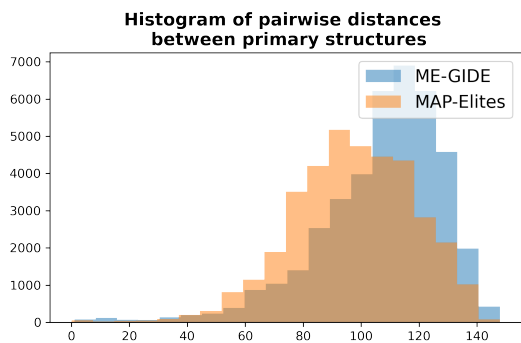
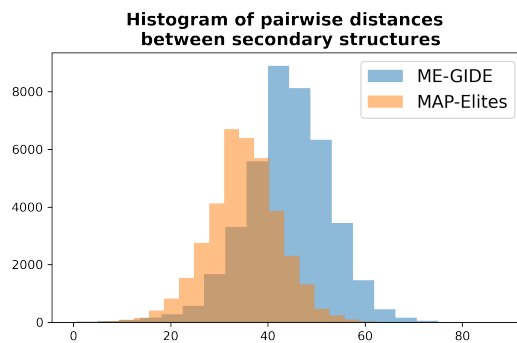


Figure 8: MNIST images projected in a t-SNE reduction of our descriptor space. The whole MNIST dataset is embedded into the 20-dimensional space defined by the PCA over the hidden units of the RBM. Then we obtain a 2-dimensional representation with t-SNE and we sample images uniformly in this space.



(a) Histogram of edit distances between sequence data over the ME-GIDE and MAP-ELITES repertoires.



(b) Histogram of edit distances between secondary structure over the ME-GIDE and MAP-ELITES repertoires.

Figure 9: ME-GIDE finds more diverse solutions in the sequence space.

## F PSEUDO-CODE FOR THE BASELINES

---

### Algorithm 3: MAP-ELITES

---

**Given:** the number of cells  $M$  and tessellation  $\mathcal{T}$ ; the batch size  $B$  and the number of iterations  $N$ ; the descriptors function  $c$  and the multi-objective function  $f$ .

```
// Initialization
For each initial solution, find the cell corresponding to its descriptor
and add initial solutions to their cells.

// Main loop
for 1 ≤ n_steps ≤ N do
  // Select new generation
  Sample uniformly B solutions x_n in the repertoire with
  replacement

  // Randomly mutate
  Sample mutants x'_n by randomly flipping one dimension.
  // Addition in the archive
  Add each mutant in its corresponding cell if it improves the cell
  fitness, otherwise discard it.
end
```

---

### Algorithm 4: Projected Objective and Measure Gradient MAP-Elites via Gradient Arborescence (OMG-MEGA (PROJ.))

---

**Given:** the number of cells  $M$  and tessellation  $\mathcal{T}$ ; the batch size  $B$  and the number of iterations  $N$ ; the descriptors function  $c$  and the multi-objective function  $f$ ; the initial population of solution candidates  $\{x_k\}$ ; the standard deviation of the gradient weights  $\sigma_g$ ;

```
// Initialization
For each initial solution, find the cell corresponding to its descriptor
and add initial solutions to their cells.

// Main loop
for 1 ≤ n_steps ≤ N do
  // Select new generation
  Sample uniformly B solutions x_n in the repertoire with
  replacement

  // Compute the gradients
  Randomly draw weights w^(n) ~ N(0, sigma_g I)
  Compute gradients nabla_{x_n} f(x_n) and nabla_{x_n} c(x_n)
  Normalize the gradients.
  Compute combined updates
  nabla_n = |w_0^(n)| nabla_{x_n} f(x_n) + sum_{i=1}^n w_i^(n) nabla_{x_n} c_i(x_n)

  // OMG-MEGA emitter
  x'_n = x_n + nabla_n
  // Project on the discrete space.
  x'_n = proj(x'_n)
  // Addition in the archive
  Add each mutant in its corresponding cell if it improves the cell
  fitness, otherwise discard it.
end
```

---



---

### Algorithm 5: Projected Covariance Matrix Adaptation MAP-Elites (CMA-MAP-ELITES (PROJ.))

---

**Given:** the number of cells  $M$  and tessellation  $\mathcal{T}$ ; the batch size  $B$  and the number of iterations  $N$ ; the descriptors function  $c$  and the multi-objective function  $f$ ; the initial population of solution candidates  $\{x_k\}$ ; the population of emitters  $E$ ; the initial standard deviation of the covariance matrices  $\sigma_0$ .

```
// Initialization
Initialize CMA emitters with the parameter sigma_0. For each initial
solution, find the cell corresponding to its descriptor and add
initial solutions to their cells.

// Main loop
for 1 ≤ n_steps ≤ N do
  // Select new generation by sampling B solutions
  (x'_n)_{1 ≤ i ≤ B} using CMA emitters
  for 1 ≤ i ≤ B do
    Select emitter e_i from E which has generated the least
    solutions out of all emitters in E.
    Unpack mean m_i and covariance matrix C_i from e_i.
    Draw a candidate from the emitter (x'_n)_i ~ N(m_i, C_i).
  end

  // Project on the discrete space.
  x'_n = proj(x'_n)
  // Addition in the archive
  Add each mutant in its corresponding cell if it improves the cell
  fitness, otherwise discard it.

  // Update of the emitters
  Update the parameters of the CMA emitters, their mean m and
  their covariance matrix C.
end
```

---